AcrAB , the major RND -type efflux pump of Photorhabdus laumondii , confers intrinsic multidrug-resistance and contributes to virulence in insects

Linda Hadchity, Anne Lanois, Paloma Kiwan, Fida Nassar, Alain Givaudan, Ziad Abi Khattar

environmental microbiology
environmental microbiology reports

AcrAB, the major RND-type efflux pump of *Photorhabdus laumondii*, confers intrinsic multidrug-resistance and contributes to virulence in insects

Journal:	*Environmental Microbiology and Environmental Microbiology Reports*
Manuscript ID	Draft
Journal:	Environmental Microbiology
Manuscript Type:	EMI - Research article
Date Submitted by the Author:	n/a
Complete List of Authors:	Hadchity, Linda; Lebanese University Faculty of Science, Life and Earth Sciences; University of Montpellier Faculty of Sciences Lanois, Anne; University of Montpellier Faculty of Sciences Kiwan, Paloma; Lebanese University Faculty of Science, Life and Earth Sciences Nassar, Fida; Lebanese University Faculty of Science, Life and Earth Sciences Givaudan, Alain; University of Montpellier Faculty of Sciences Abi Khattar, Ziad; Lebanese University Faculty of Science, Life and Earth Sciences
Keywords:	Photorhabdus laumondii, RND efflux pumps, AcrRAB, MdtABC, MDR, Insects, Virulence

AcrAB, the major RND-type efflux pump of *Photorhabdus laumondii,* confers intrinsic multidrug-resistance and contributes to virulence in insects

Linda Hadchity[1,2], Anne Lanois[2], Paloma Kiwan[1], Fida Nassar[1], Alain Givaudan[2*], Ziad Abi Khattar[1*]

[1] Laboratory of Georesources, Geosciences and Environment (L2GE), Microbiology/Tox-Ecotoxicology team, Faculty of Sciences 2, Lebanese University, Fanar, Lebanon.

[2] DGIMI, Université Montpellier, INRAE, Montpellier, France.

* Ziad Abi Khattar

L2GE, Department of Life and Earth Sciences, Faculty of Sciences 2, Lebanese University

P.O.Box 90656, Jdeideh, Fanar-Lebanon

Telephone: +96171771703

Fax: +961680250

Email: ziad.abikhattar@ul.edu.lb

* Alain Givaudan

UMR DGIMI 1333 INRA, Université de Montpellier, Bât 24 3ème étage, Place Eugène Bataillon CC54, 34095, Montpellier Cedex 5-France

Telephone: +33467144812

Fax: +33467144299

Email: alain.givaudan@umontpellier.fr

Author emails: linda.hadchity@etu.umontpellier.fr; anne.lanois-nouri@umontpellier.fr; paloma.kiwan.1@st.ul.edu.lb; fida.nassar@ul.edu.lb; alain.givaudan@umontpellier.fr; ziad.abikhattar@ul.edu.lb

Abstract

The resistance-nodulation-division (RND)-type efflux pumps AcrAB and MdtABC contribute to multidrug-resistance (MDR) in Gram-negative bacteria. *Photorhabdus* is a symbiotic bacterium of soil nematodes that also produces virulence factors killing insects by septicaemia. We previously showed that *mdtA* deletion in *Photorhabdus laumondii* TT01 resulted in no detrimental phenotypes. Here, we investigated the roles of the last two putative RND transporters in TT01 genome, AcrAB and AcrAB-like (Plu0759-Plu0758). Only Δ*acrA* and Δ*mdtA*Δ*acrA* mutants were multidrug sensitive, even to triphenyltetrazolium chloride and bromothymol blue used for *Photorhabdus* isolation from nematodes on the NBTA medium. Both mutants also displayed slightly attenuated virulence after injection into *Spodoptera littoralis*. Transcriptional analysis revealed intermediate levels of *acrAB* expression *in vitro, in vivo* and post-mortem, whereas its putative transcriptional repressor *acrR* was weakly expressed. Yet, plasmid-mediated *acrR* overexpression did not decrease *acrAB* transcript levels neither MDR in TT01 WT. While no pertinent mutations were detected in *acrR* of the same *P. laumondii* strain grown either on NBTA or nutrient agar, we suggest that AcrR-mediated repression of *acrAB* is not physiologically required under conditions tested. Finally, we propose that AcrAB is the primary RND-efflux pump which is essential for MDR in *Photorhabdus* and may confer adaptive advantages during insect infection.

Introduction

Entomopathogenic bacteria of the genus *Photorhabdus* are Gram-negative, bioluminescent and motile rods comprising the widely studied type strain *P. laumondii* TT01 (Boemare, 2002; Duchaud *et al.,* 2003; Machado *et al.,* 2018). *Photorhabdus* and its sister genus *Xenorhabdus* formerly classified as *Enterobacteriaceae* were recently considered as part of the family *Morganellaceae* (Adeolu *et al.,* 2016). *P. laumondii* is mutualistically associated with the gut of *Heterorhabditis bacteriophora* infective juvenile (IJ) nematodes which are alternative non-feeding free L3 stage larvae, capable of infecting a broad range of soil-dwelling insect larvae (Stock and Kaya, 1996; Boemare, 2002). Upon reaching insect haemolymph, IJs regurgitate *Photorhabdus* that then kill the insect by septicaemia after bioconverting its internal tissues and organs into a nutrient soup. This microhabitat provides a protected niche to bacteria and nematodes where they feed off (Ciche and Ensign, 2003). Meanwhile, IJs triggered by food signals produced by bacteria in the stationary phase, undergo a developmental process recovering them into self-fertile adult hermaphrodite nematodes that undergo many reproduction cycles (Strauch and Ehlers, 1998; Johnigk and Hlers, 1999). The destruction of the IJ recovery signal originally present in haemolymph and the deterioration of the insect cadaver conditions along with the increasing nematode populations cause IJs to leave the cadaver and to spread in the soil, looking for a new insect host (Clarke, 2020). For the selective isolation of *Photorhabdus* from IJ nematodes, NBTA medium has been developed and consists of nutrient agar supplemented with bromothymol blue (BTB) and triphenyltetrazolium chloride (TTC), allowing to differentiate between the primary and secondary forms of *Photorhabdus* based on BTB absorption and/or TTC reduction (Akhurst, 1980).

Due to the great versatility of *Photorhabdus* in transitioning from a virulence correlated-exponential growth phase in insects to a mutualistic post-exponential (stationary) growth phase in nematodes (Clarke, 2020), these bacteria must be able to avoid and/or cope with different stress conditions during their life cycle. Indeed, the success of *Photorhabdus* as an insect pathogen depends on many virulence factors (Nielsen-LeRoux *et al.,* 2012). One of the most relevant virulence strategies of *Photorhabdus* is resistance to killing by circulating cationic antimicrobial peptides (AMPs) whose production by the insect fat body is rapidly induced upon bacterial entry into the haemolymph (Eleftherianos *et al.,* 2010; Mouammine *et al.,* 2017). This rapid adaptation to AMPs mainly results from LPS modifications mediated by the *pbgPE* operon in a PhoP-dependent manner (Derzelle *et al.,* 2004; Bennett and Clarke, 2005), and was shown to be driven by a minor AMP resistant subpopulation of *P. laumondii* causing septicaemia in insects (Mouammine *et al.,* 2017).

Active efflux as a mechanism for bacterial resistance to toxic compounds mediated by MDR efflux pumps is among the most relevant virulence and/or stress adaptation strategies in bacteria (Martinez *et al.,* 2009; Du *et al.,* 2018). MDR pumps are, with few exceptions, chromosomally encoded membrane-associated proteins that can extrude a wide range of bacterial products and xenobiotics therefore conferring core functions and intrinsic antibiotic resistance to bacteria (Du *et al.,* 2018). Bacterial drug efflux pumps could be classified into six superfamilies / families comprising the ATP-binding cassette (ABC) family and five other secondary active transporters powered by electrochemical energy captured in transmembrane ion gradients: the major facilitator superfamily (MFS), the multidrug and toxin extrusion (MATE) family, the small multidrug resistance (SMR) family, the proteobacterial antimicrobial compound efflux (PACE) family and the resistance-nodulation-cell division (RND) superfamily (Du *et al.,* 2018). RND-type

drug efflux pumps are common in Gram-negative bacteria and consist of an inner membrane pump, a periplasmic adaptor protein and an outer membrane protein channel. These transporters extrude an array of structurally diverse substrates, including biocides and antibiotics, from the periplasm / outer leaflet of the inner membrane to the outside of the cell thus providing intrinsic MDR to many clinically relevant Gram-negative bacterial species (Colclough *et al.,* 2020). Moreover, RND efflux pumps are involved in the export of toxic molecules of host origin such as bile salts (Nishino *et al.,* 2006), AMPs and fatty acids (Bina *et al.,* 2008; Joo *et al.,* 2016; Leus *et al.,* 2018), as well as many bacterial metabolites like amino acids (Cauilan *et al.,* 2019), toxins (Kang and Gross, 2005), siderophores (Horiyama and Nishino, 2014; Kunkle *et al.,* 2017), and quorum sensing molecules (Lee and Zhang, 2015). AcrAB-TolC, the paradigm RND efflux pump of *Enterobacteria,* was extensively studied in *E. coli* and *Salmonella* (Li and Nikaido, 2016; Nishino, 2016). AcrB is a homotrimer drug-proton antiporter with multiple active binding sites in the porter region accounting for the substrate polyselectivity, acting as a tripartite complex with the outer membrane channel TolC and the periplasmic adapter protein AcrA (Kobylka *et al.,* 2020). The *acrAB* operon is transcribed divergently from the local *acrR* gene encoding a transcriptional repressor that binds to the AcrR-binding motif overlapping the *acrAB* promoter (Deng *et al.,* 2013). Induction of *acrAB* is therefore achieved through ligand binding to AcrR. These inducible ligands are often antibiotic substrates of AcrAB such as cationic dyes and ciprofloxacin (Li *et al.,* 2007; Deng *et al.,* 2013). Moreover, increased efflux could be attained following direct or indirect induction of *acrAB* transcription by a complex network of two component system and global regulators namely MarA, SoxS, Rob, EvgA, SdiA, and CpxR in response to environmental signals as for example noxious substances or stressors (Du *et al.,* 2018; Weston *et al.,* 2018). The AcrAB-TolC efflux system is known to be responsible for the extrusion of a broad range of compounds

including lipophilic antimicrobial drugs, antibiotics, various dyes, detergents, and organic solvents thus conferring MDR in many Gram-negative bacteria like *E. coli*, *Salmonella, Klebsiella*, *Erwinia,* and *Acinetobacter* (Colclough *et al.,* 2020). More importantly, AcrAB-TolC contributes to bacterial virulence by impacting biofilm formation, host-cell invasion and colonization abilities of several bacterial pathogens in plant and animal models of infection (Alav *et al.,* 2018; Colclough *et al.,* 2020). AcrAB-TolC defective mutants of *Salmonella* Typhimurium and *Erwinia amylovora* were remarkably sensitive to host-produced molecules in particular bile salts, fatty acids and flavonoids, also acting as inducing signals of *acrAB-tolC* expression (Burse *et al.,* 2004; Baucheron *et al.,* 2014). The AcrAB-TolC pump was also shown to impact metabolism at a global scale by regulating the intra/extracellular levels of central metabolism intermediates in *E. coli* (Cauilan *et al.,* 2019).

To date, no functional data are available for MDR efflux pumps in *Photorhabdus* species. Our previous report on RND transporters in *P. laumondii* showed that the MdtABC efflux pump expression is highly induced within insect connective tissues in a protease-dependent manner during late stages of infection (Abi Khattar *et al.,* 2019). Even though no clear phenotypes were related to MdtABC in *Photorhabdus*, we suggested that RND pumps may be involved in bacterial adaptation and survival to adverse conditions experienced in the cadaver prior to *Photorhabdus* transmission to IJ nematodes (Abi Khattar *et al.,* 2019).

Herein, we uncovered the first key role of a RND efflux pump, AcrAB-TolC, in intrinsic MDR of *P. laumondii* as well as a contribution of this transporter to bacterial virulence in insects. We showed that *acrA* mutation has significantly reduced resistance to several antibiotics, detergents, AMPs, and unexpectedly to BTB and TTC, currently used as differential dyes in the selective isolation of *Photorhabdus* from nematodes. We also revealed a substrate-specific cooperative

efflux between AcrAB and MdtABC which enhanced resistance to BTB, novobiocin and sodium deoxycholate (DOC). Transcriptional approaches by RT-qPCR and GFP reporter gene expression indicated that *acrA* promoter is constantly active *in vitro* and *in vivo* in a tissue-independent manner all over the infection process until early post-mortem stages within the insect cadaver. Overexpression of the *acrR* local repressor gene did not lower *acrAB* transcript level neither MDR in TT01 WT. Nucleotide sequence alignment for five strains of *P. laumondii* exposed or not to BTB and TTC did not reveal any mutations in *acrR* gene or the AcrR-binding motif, suggesting that AcrR-mediated repression of *acrAB* in *P. laumondii* TT01 is not physiologically required under conditions tested. Finally, mutation of the *P. laumondii plu0759* gene encoding the putative periplasmic adapter protein of the AcrAB-like Plu0759-Plu0758 efflux pump had no detectable phenotypes with respect to the WT strain, leading to the conclusion that the AcrAB efflux pump plays the most relevant role in MDR among all RND transporters in *P. laumondii*.

Results

Genomic environment of the *acrRAB*, *tolC* and *plu0751-plu0765* loci in *Photorhabdus laumondii* TT01 genome

In silico analysis of the *P. laumondii* TT01 genome sequence revealed the presence of a putative *acrAB* efflux pump operon closely homologous to that of *E. coli*. This locus includes the *acrA* gene (*plu3851*) putatively encoding the « *acriflavin resistance protein A precursor »* serving as the periplasmic adaptor protein AcrA (84 % similar to AcrA of *E. coli*) followed by the *acrB* gene (*plu3852*) that encodes the « *acriflavin resistance protein B »* sitting as the inner membrane RND protein AcrB (90 % similar to AcrB of *E. coli*). In *E. coli*, AcrAB recruits the outer membrane channel TolC (81% similar to TolC of *E. coli*) encoded by the *plu3954* gene, located elsewhere in

P. laumondii TT01 genome. The *acrR* gene (*plu3850*), located upstream and in the opposite direction of the *acrA* gene, encodes AcrR, a putative transcriptional repressor of *acrAB* sharing 78% of similarity with the well-studied AcrR from *E. coli*. The *acrRAB* locus exhibited very well-conserved structure and arrangement within genomes of *Photorhabdus* species and those of the sister genus *Xenorhabdus*, *E. coli* and *S.* Typhimurium. Comparison of genomic regions surrounding *acrRAB* and *tolC* genes from different enterobacterial species showed a global synteny conservation, although the *kefA* gene encoding a potassium efflux system is lacking in *Photorhabdus* (Fig. 1A). In light of the high amino acid sequence similarity of the AcrAB-TolC proteins from *P. laumondii* and *E. coli*, the *acrRAB-tolC* genes probably belong to the core genome and encode a tripartite AcrAB-TolC export system in *Photorhabdus*. Moreover, the genomic organization of the *acrAB* genes suggests a polycistronic transcription which was confirmed by RT-qPCR showing that *acrA* mutation had a polar effect on the downstream *acrB* RNA amount but not on the histone-like *hha* located at 1055 bp relative to the *acrB* ORF stop codon (Fig. S1). In *Photorhabdus*, *acrR* and *acrA* genes are transcribed divergently from the same 129 bp *acrR-acrA* intergenic region harbouring the *acrR* and *acrAB* promoters (Table S2). The latter consists of a 24 bp inverted repeat sequence located at position -77 (TACATACATTCACGTATGTTTGTA) relative to the start codon of *acrA* ORF which is thought to be the AcrR-binding motif in *Photorhabdus* (Fig. S2A and S2B), as previously shown in *E. coli* (Su *et al.,* 2007).

Moreover, analysis of *P. laumondii* TT01 genome sequence revealed the presence of an additional putative RND efflux pump locus, *plu0758-plu0759*, encoding proteins with similarities to multidrug efflux membrane fusion proteins serving as the periplasmic adaptor protein and a protein similar to multidrug efflux transporter, respectively. The Plu0759 protein is 39 % similar

to AcrA of *P. laumondii* TT01, 37 % similar to AcrA of *E. coli* K12, 40 % similar to MdtA of *P. laumondii* TT01 and *P. luminescens* DSM 3368, and 39 % similar to MdtA of *E. coli* K12. The *plu0759* gene is followed by the *plu0758* gene which putatively encodes a product similar to multidrug efflux transporters from *P. laumondii* TT01 and *P. luminescens* DSM 3368 (52 %, 50 %, and 49 % similar to AcrB, MdtB, and MdtC, respectively), *Xenorhabdus nematophila* ATCC19061, *E. coli* K12 and *S.* Typhimurium LT2 (51 %, 49 %, and 49 % similar to AcrB, MdtB, and MdtC, respectively). Furthermore, the KEGG database resource search revealed that the *plu0759* and *plu0758* genes are, respectively, *acrA*/*mdtA* and *acrB*/*mdtB*/*mdtC* paralogs, encoding a putative RND efflux pump which we propose to annotate as AcrAB-like. Interestingly, the AcrAB-like encoding genes are located close to a putative MATE-like efflux pump-encoding *plu0761* gene, within a 17.27 kb *plu0751-plu0765* genomic cluster (Fig. 1B). All other *Photorhabdus* genomes lacked the *plu0751-plu0765* region except all other *P. laumondii* (HP88 and IL9) and some *P. luminescens* (DSM3368 and BA1) (https://www.mage.genoscope.cns.fr/agc/mage) suggesting that this region may belong to the plastic genome (Fig. 1B).

acrAB mutation decreases intrinsic resistance to exogenous toxic compounds

We investigated the roles of all three RND efflux pumps of *P. laumondii* TT01 by testing the Δ*acrA*, Δ*mdtA*Δ*acrA* and Δ*acrA*-like mutants for several cultural traits of *Photorhabdus* genus as well as for antimicrobial sensitivity. First, the *in vitro* growth of mutant strains was assessed in the routinely used LB broth at 28˚C. Δ*acrA*, Δ*mdtA*Δ*acrA* and Δ*acrA*-like mutants grew similarly to the TT01 WT strain (Fig. S3), thus indicating that none of these mutations resulted in any detectable *in vitro* growth defect. Moreover, bacterial plating has been performed on NBTA

medium on which the TT01 WT bacteria typically grow into blue-green colonies, as they absorb the BTB dye (Akhurst, 1980). Surprisingly, both Δ*acrA*/pBBR1-MCS5 and Δ*mdtA*Δ*acrA*/pBBR1-MCS5 mutants exhibit no growth on NBTA agar in contrast to that of Δ*acrA*-like. This phenotype was reverted in the *acrAB*-complemented Δ*acrA* and Δ*mdtA*Δ*acrA* mutants (Table 1 and Fig. S4). The *mdtABC*-complemented Δ*acrA* and Δ*mdtA*Δ*acrA* mutants exhibited normal growth patterns only on a TTC free-NBTA medium (i.e, nutrient agar + BTB) and their cultural characteristics were identical to those of the parental TT01 strain (Table 1). These findings underlined the requirement of the AcrAB efflux pump for growth of *P. laumondii* on NBTA agar, and led us to curiously investigate whether any of the NBTA constituents, BTB dye and/or the TTC redox indicator, could have a deleterious impact on the growth of these mutants. The Δ*acrA*/pBBR1-MCS5, Δ*mdtA*Δ*acrA*/pBBR1-MCS5, Δ*acrA*/pBBR1-*mdtABC*, and Δ*mdtA*Δ*acrA*/pBBR1-*mdtABC* strains showed an impaired growth on a BTB-free NBTA medium (i.e, nutrient agar + TTC) (Table 1). We then evaluated the mutant susceptibility to BTB and TTC by determining the MICs of these compounds for the different bacterial strains. As shown in table 1, Δ*acrA* and Δ*mdtA*Δ*acrA* mutants were more susceptible to BTB and TTC than the parental strain while the Δ*acrA*-like and TT01 strains had similar susceptibility levels to these compounds. The BTB MICs were restored when mutant strains were complemented *in trans* with a WT copy of the *acrAB* or *mdtABC* operons while the TTC MICs were restored only when mutant strains were complemented with a WT copy of the *acrAB* operon. As regards to the Δ*acrA*/pBBR1-MCS5 simple mutant, the Δ*mdtA*Δ*acrA*/pBBR1-MCS5 double mutant showed a 4-fold decrease of BTB MIC while no difference in TTC MICs was observed. This further confirmed the relative hypersusceptibility of the double mutant to BTB compared to the simple mutant. These results corroborate somewhat the observations made on NBTA medium with MdtABC alone allowing 8 and 31-fold increase of

BTB MIC for simple Δ*acrA* and double Δ*mdtA*Δ*acrA* mutants, respectively (Table 1). Therefore, these data outstandingly showed that AcrAB is essential for resistance to TTC and that full resistance to BTB requires both AcrAB and MdtABC in *P. laumondii* (Table 1 and Fig. S4).

We also determined the MICs of typical antimicrobials, but also non-antibiotic substrates of the AcrAB-TolC efflux pump for the different bacterial strains, such as lipophilic antimicrobial drugs (novobiocin and macrolides), fluoroquinolone and cephalosporin antibiotics, AMPs (linear cecropins and polycyclic polymyxins), dyes (ethidium bromide, EtBr), bile salts (DOC) and detergents (sodium dodecyl sulfate, SDS). As shown in Table 2, both Δ*acrA* and Δ*mdtA*Δ*acrA* were multidrug and dye susceptible when compared to the parental strain, while Δ*acrA*-like and TT01 WT had similar susceptibility levels to all common AcrAB substrates. Indeed, the MICs of novobiocin, erythromycin, polymyxin B, colistin (polymyxin E), SDS, DOC, and EtBr variably decreased from 8 to 2083-fold for Δ*acrA*/pBBR1-MCS5 and Δ*mdtA*Δ*acrA*/pBBR1-MCS5, with reference to the WT TT01/pBBR1-MCS5 strain. The double mutant Δ*mdtA*Δ*acrA*/pBBR1-MCS5 was more susceptible than the simple mutant Δ*acrA*/pBBR1-MCS5 to novobiocin (10-fold) and DOC (8-fold). The double mutant hypersusceptibility to novobiocin and DOC was confirmed by a partial restoration of the parental phenotype after complementation with the WT *mdtABC* operon (0.5 µg.mL^{-1} and 488 µg.mL^{-1}, respectively), and a full restoration after complementation with the parental *acrAB* operon. These results emphasized a cooperative efflux between AcrAB and MdtABC in order to enhance resistance to novobiocin and DOC. However, TT01 WT, Δ*acrA*, Δ*mdtA*Δ*acrA* and Δ*acrA*-like mutant strains had similar or non-significant difference in susceptibility levels to cefuroxime, cefaclor, ceftriaxone, aztreonam, ciprofloxacin, nalidixic acid, norfloxacin, $MgSO_4$, $ZnSO_4$, $CuSO_4$, $(NH_4)_2SO_4$, saponin, uric acid, and indole (Table S1).

In contrast to the cecropins A and C, MICs of polymyxins were significantly reduced for the mutant strains comparing to those determined for the parental strain. At least, an 8-fold decrease of colistin MIC was observed for both mutants comparing to that determined for the parental strain while the MIC of polymyxin B decreased 8-fold for Δ*acrA* and 16-fold for Δ*mdtA*Δ*acrA* comparing to that determined for the parental strain. Based on EUCAST/CLSI breakpoints for colistin and CLSI cut-off values for polymyxin B (CLSI, 2017; EUCAST, 2021), such MICs are remarkably high hence categorizing both mutants as phenotypically polymyxin resistant strains. Taken together, these results highlighted that among the three RND efflux pumps identified in *P. laumondii* TT01*,* AcrAB is the major MDR transporter that extrudes, to different extents, a wide range of structurally-diverse exogenous compounds comprising bile salts, detergents, dyes, antibiotics, and polycyclic AMPs hence accounting for the intrinsic resistance of *P. laumondii*.

Expression patterns of *acrRAB* during *in vitro* bacterial growth

To assess the expression of *acrRAB* in *P. laumondii*, we first monitored GFP expression *in vitro* by calculating the specific fluorescence values overtime for *P. laumondii*-P$_{acrA}$-*gfp*'[AAV] and *P. laumondii*-P$_{acrR}$-*gfp*[AAV] transcriptional fusions under normal laboratory conditions in LB broth. At the maximum rate, recorded at between 18 and 20 hours of growth (A_{600nm} of 1), the specific fluorescence ratios of *P. laumondii*-P$_{acrA}$-*gfp*'[AAV] and *P. laumondii*-P$_{acrR}$-*gfp*[AAV] over a strain carrying P$_{lac}$-*gfp*[AAV] (Abi Khattar *et al.,* 2019) were 0.62 and 0.14, respectively. When comparing these values to "0.11" which is the value of the same ratio calculated for *P. laumondii*-P$_{mdtABC}$-*gfp*[AAV] taken as a reference in the same growth conditions (Abi Khattar *et al.,* 2019), we can say that *acrAB* is expressed at moderate levels in all phases of bacterial growth while the expression of the *acrR* repressor gene is weak (Fig. 2). Furthermore, RT-qPCR

experiments showed that the *acrA* transcripts were expressed at moderate levels in LB broth in exponential phase and slightly increased (2-fold) during stationary phase, while the *acrR* gene was expressed at very low levels in *P. laumondii* TT01 WT in both phases (Fig. S5).

AcrAB-related phenotypes are AcrR-independant in *P. laumondii* under regular laboratory conditions

In order to investigate the functionality of AcrR in regulating *acrAB* expression in *P. laumondii*, the expression of *acrR* and *acrA* genes in TT01/pBBR1-MCS5 and TT01/pBBR1-*acrR* strains were evaluated by RT-qPCR. Results showed that the rate of *acrR* transcripts in TT01/pBBR1-*acrR* was 3.48-fold greater than that in TT01/pBBR1-MCS5, indicating that *acrR* expression was successfully enhanced in TT01 WT carrying a plasmidic *acrR* copy under the P_{lac} promoter which is constitutively expressed in TT01 (Fig. 3). However, the transcript rates of *acrA* and *acrB* in TT01/pBBR1-MCS5 and TT01/pBBR1-*acrR* did not show any significant difference, meaning that AcrR is either a non-functional repressor of *acrAB* in *P. laumondii* or is inoperative under tested conditions (Fig. 3). We then investigated the functionality of *acrR* by evaluating its putative impact on AcrAB-related phenotypes such as growth on NBTA and MDR. Both TT01/pBBR1-MCS5 and TT01/pBBR1-*acrR* grew similarly on NBTA and were equally resistant to relevant drugs (Table 3), thus corroborating our transcriptional analyses.

These overall findings led us to check whether the expression of *acrAB* and the failure of AcrR to repress it, were due to AcrR mutation(s) resulting in a highly MDR *P. laumondii* strain, as previously described in *E. coli* (Webber *et al.,* 2005). That could have resulted from unwanted experimental selection occurring in the laboratory collecting *Photorhabdus* from IJ nematodes by using NBTA medium. We therefore amplified by PCR the *acrR* gene and its 24 bp IR binding

297 motif from TT01 WT and four other isolates of *P. laumondii* newly isolated from nematodes on
298 nutrient agar, and from these same strains sub-cultured previously onto NBTA. The primer set
299 used consisted of L-acrR-seq and R-acrR-seq that were designed in highly conserved regions from
300 different *Photorhabdus* strains (Table S3). DNA sequencing analyses did not reveal any relevant
301 mutation neither in the 24 bp motif nor in the *acrR* gene sequence in the same *P. laumondii* strain
302 grown either on NBTA medium or nutrient agar (Fig. S6). Taken together, these data suggest that
303 AcrR is not an effective *acrAB* repressor in *P. laumondii* under our tested conditions.
304

305 **The *acrAB* operon is expressed *in vivo* and involved in bacterial virulence towards insects**
306 Monitoring the expression of *acrAB* and *acrR* promoter-*gfp* fusions during *S. littoralis* infection
307 revealed that *acrAB* promoter was moderately active in both haemolymph (Fig. 4A and 4B) and
308 mid-gut connective tissues (Fig. 4C and 4D) as soon as septicaemia was established at 20 to 24
309 hours post-injection (hpi), and within the insect cadaver during the early post-mortem period (Fig.
310 4E and 4F). Such an expression profile could provide immediate benefits when AcrAB proteins
311 are needed in order to efficiently cope with the ever-changing environment of the infected insect.
312 Indeed, intrahaemocoel injection of *S. littoralis* larvae with *P. laumondii* strains revealed that the
313 LT_{50} was reached after 35.6, 44, and 40.4 hpi of the TT01 WT, Δ*acrA,* and Δ*mdtA*Δ*acrA* strains,
314 respectively. Statistical analysis confirmed that the Δ*acrA* and Δ*mdtA*Δ*acrA* mutants were slightly
315 less virulent than the WT even though the Δ*acrA* exhibited a 3.6 hour delay in the LT_{50} comparing
316 to the Δ*mdtA*Δ*acrA* ($P = 0.002$) (Fig. 5). Additionally, the LT_{50} decreased by 3 and 6 hours when
317 injecting the *acrAB*-complemented Δ*acrA* mutant with reference to the WT TT01/pBBR1-MCS5
318 and Δ*acrA*/pBBR1-MCS5 strains, respectively (Fig. S7).

The MICs of insect AMPs (cecropin A and C, Table 2) were equal for both TT01 WT and mutant strains. Therefore, considering our previous findings that the AMP/polymyxin resistant subpopulation of *P. laumondii* TT01 is responsible for virulence in insects (Mouammine *et al.,* 2017), we estimated the percentage of polymyxin B resistant population by plating TT01 WT and *acrA* mutant strains on nutrient agar supplemented or not polymyxin B (100 $\mu g.mL^{-1}$). Plate counts did not disclose any significant difference between percentages of the WT, the Δ*acrA* and the Δ*mdtA*Δ*acrA* polymyxin B resistant populations (about 0.3 to 0.4 %), suggesting that the involvement of the AcrAB efflux pump of *P. laumondii* in insect virulence is not related to AMP resistance.

Discussion

RND efflux pumps appear to be evolutionarily ancient elements, highly relevant for the physiology and ecological behavior of Gram-negative bacteria (Colclough *et al.,* 2020). The genome sequence of *P. laumondii* TT01 enabled us to trace three putative RND-type drug efflux loci, *mdtABC*, *acrAB* and *acrAB*-like. While the *acrRAB* are highly conserved genes belonging to the core genome of Gram-negative bacterial taxons (Annunziato, 2019), the accessory *acrAB*-like genes were detected only in all *P. laumondii* and some *P. luminescens* sub-species (https://www.mage.genoscope.cns.fr/agc/mage) suggesting that they have evolved by horizontal genetic transfer. In *E. coli* and *Salmonella*, the number of functional multidrug transport (*mdt*) and acriflavin (*acr*) efflux pump paralogs reached five (Anes *et al.,* 2015; Blair *et al.,* 2015), while twelve RND-type multidrug efflux pump genes were recently characterized in *Klebsiella pneumoniae* (Ni *et al.,* 2020). The number of MDR efflux pumps is proportional to the genome size of a given organism which in turn depends on bacterial ecological behavior (Mira *et al.,* 2001;

342 Ren and Paulsen, 2005). Although *Photorhabdus* has a significantly larger genome size compared
343 with other *Morganellaceae* and *Enterobacteriaceae* (http://www.ncbi.nlm.nih.gov/genome), it
344 possesses the lowest repertoire of RND efflux pump genes. This may seem surprising in view of
345 its complex interactions as mutualistic, saprophytic and pathogen, its host specificity and particular
346 stress encountered in its life cycle.

347 Our previous study could not assign a clear phenotype to *mdtABC* mutation but revealed
348 that other RND transporters may contribute to MDR in *P. laumondii* (Abi Khattar *et al.,* 2019).
349 We showed here that AcrAB efflux pump is essential for intrinsic resistance to many structurally
350 unrelated compounds including lipophilic antibiotics, bile salts, detergents, dyes, and polymyxins
351 B and E (colistin), most of which are common substrates of RND efflux pumps (Trimble *et al.,*
352 2016; Colclough *et al.,* 2020). We also provided the first evidence that MdtABC efflux pump
353 contributes to *P. laumondii* multiresistance by sharing overlapping substrate specificity with
354 AcrAB for novobiocin and DOC, which is in good agreement with previous reports in *E. coli*,
355 *Salmonella* and *Erwinia* (Nagakubo *et al.,* 2002; Nishino et al., 2006; Pletzer and Weingart, 2014).
356 Another important finding of our study is that MdtABC does not replace AcrAB function under
357 conditions tested but only partially compensates for its deficiency.
358 On the other hand, inactivation of the *acrAB* paralog, named *acrAB*-like, had no effect whatsoever
359 and even failed to complement the Δ*acrA* mutant for resistance to toxic compounds (Hadchity, L.
360 unpublished). It is clear that pumps can function on a variety of substrates, and sequence changes
361 can impact functional identity leading to changes in substrate specificity (Nazarov *et al.,* 2020).
362 This suggests that AcrAB and AcrAB-like of *P. laumondii* are genetic but not functional paralogs,
363 with AcrAB-like pump possibly having a narrower substrate range providing it with yet
364 unrecognized functions in *Photorhabdus*.

Since the 1980s, isolation and detection of the bacterium *Photorhabdus* from IJ nematodes in all laboratories working on entomopathogenic nematodes is conventionally performed on the selective BTB and TTC-containing NBTA medium. In addition, BTB dye and TTC redox indicator allow discrepancy between two variant forms of *Photorhabdus* based on colony morphology: variant 1 which exhibits dark blue colonies by absorbing BTB and reducing TTC and variant 2 developing red colonies after reducing TTC (Akhurst, 1980). We unexpectedly showed that growth on NBTA medium essentially requires AcrAB for resistance to TTC along with a functional MdtABC working cooperatively to confer BTB resistance. TTC seems to be a unique substrate of AcrAB in *Photorhabdus* not yet reported for other bacteria, and consequently, *Photorhabdus* sensitivity to TTC is an evidence of a non-functional AcrAB efflux pump. Thus, we assumed that isolation of *Photorhabdus* on the NBTA medium could be inadvertently selected for strains with functional AcrAB and so are all strains currently maintained and being studied in laboratories worldwide. This is the reason why we depicted *acrAB* expression in *P. laumondii*. Bacteria are able to employ multidrug efflux pumps in a very efficient, precise, and complex way by specifically regulating the expression of the drug transporter genes (Du *et al.,* 2018). Indeed, RND efflux pump expression is frequently down-regulated except for *acrAB* genes displaying a substantial expression level under regular laboratory growth conditions (Alcalde-Rico *et al.,* 2016). Reporter gene fusions and RT-qPCR transcriptional analyses in *P. laumondii* revealed that the expression of *acrAB* is stable at moderate levels during exponential- and stationary-phases under regular growth conditions *in vitro.* Such expression patterns are compatible with those previously reported in *E. coli* (Kobayashi *et al.,* 2006). The expression of *acrAB* slightly increased as *Photorhabdus* entered the stationary phase suggesting a potential role of AcrAB in adaptation to stationary phase stress responses, as previously described in *E. coli* (Rand *et al.,* 2002). In

388 clinically relevant enterobacteria, the transcription of *acrAB* genes is globally up-regulated by
389 stress response activators MarA, Rob, SoxS, SdiA and RamA (Bailey *et al.,* 2010; Duval and
390 Lister, 2013), and locally down-regulated by the specific AcrR repressor (Olliver *et al.,* 2004; Su
391 *et al.,* 2007). In an attempt to functionally analyze the effect of AcrR in *P. laumondii*, we showed
392 that plasmid-mediated *acrR* overexpression had no effect on *acrAB* expression neither on AcrAB-
393 mediated phenotypes. Regulatory gene mutations associated with *acrAB* overexpression were
394 frequently detected in *acrR* sequences of various bacteria with increased levels of resistance to
395 several unrelated antibiotics (Olliver *et al.,* 2004; Webber *et al.,* 2005; Deng *et al.,* 2013; Jaktaji
396 and Jazayeri, 2013). The effect of these mutations on *acrAB* overexpression was shown to be
397 dependent on the levels of resistance to some antibiotics in *E. coli* (Jaktaji and Jazayeri, 2013).
398 Yet, no relevant mutations were detected in *acrR* gene and promoter sequences from the same *P.*
399 *laumondii* strain grown either on nutrient agar or on NBTA medium. Therefore, it is likely that
400 AcrR repressor is ineffective in *Photorhabdus* under routine *in vitro* growth conditions, in the seek
401 to maintain a trade-off between *acrAB* expression and bacterial relative fitness.

402 The expression level of efflux pumps can significantly impact bacterial virulence in
403 experimental infection models (Colclough *et al.,* 2020). Unlike the tissue-specific induction of
404 *mdtABC* during late infection stages (Abi Khattar *et al.,* 2019), the *acrAB* promoter in *P. laumondii*
405 was moderately active in both haemolymph and connective tissues throughout the infection
406 process. This activity was maintained within the insect cadaver as previously reported for *mdtABC*
407 (Abi Khattar *et al.,* 2019), raising the possibility that these pumps have potential roles in bacterial
408 behavior and detoxifying natural compounds encountered *in vivo.* In an AcrB loss-of-efflux-
409 function mutant of *Salmonella*, *phoPQ* genes were significantly downregulated, which was likely
410 the cause of the attenuated virulence of this mutant in mouse and *Galleria mellonella* models

411 (Wang-Kan *et al.,* 2017). In *Photorhabdus*, PhoP-dependent modification of LPS by an AMP
412 resistant bacterial subpopulation is the most powerful virulence strategy responsible of killing
413 insect by septicaemia (Derzelle *et al.,* 2004; Mouammine *et al.,* 2017). We showed here that
414 *acrAB*-deficient mutants of *Photorhabdus* had no growth defects and were highly resistant to
415 AMPs *in vitro* including insect-derived cecropin C (Duvic *et al*., 2012; Huot *et al*., 2019), while
416 also being able to successfully cause septicaemia in insects. Thus, the slight impact of *acrAB*
417 mutation on *Photorhabdus* virulence was not correlated to increased AMP sensitivity in
418 haemolymph. In line with this finding, AcrAB seems to indirectly contribute to AMP tolerance at
419 supra-physiological concentrations, most probably by maintaining membrane integrity rather than
420 direct efflux, which is definitely irrelevant for *Photorhabdus* ability to resist AMP-killing in the
421 haemolymph. Other hypotheses must therefore be considered in order to explain the attenuated
422 phenotype of the Δ*acrA* mutant. The expression of *acrAB* in *E. coli* is upregulated in response to
423 cellular metabolites including those related to cysteine, purine and the siderophore
424 enterobactin biosynthesis, which are also extruded by AcrB, AcrD and MdtABC pumps
425 (Horiyama and Nishino, 2014; Ruiz and Levy, 2014). AcrAB or its homologues were also shown
426 to be required for optimal production of virulence factors (Burse *et al.,* 2004; Bina *et al.,* 2008;
427 Wang-Kan *et al.,* 2017) and biofilm formation (Alav *et al.,* 2018). However, AcrAB mutants of
428 *Photorhabdus* were not impaired in their ability to form biofilm *in vitro* (Hadchity, L.
429 unpublished). Recently, a metabolomic-based study in *E. coli* confirmed that TolC-dependent
430 pumps play an important role in cell metabolism by demonstrating that AcrAB pump deletion or
431 overproduction was associated with changes in a large number of central metabolism intermediates
432 (Cauilan *et al.,* 2019). Therefore, the accumulation of such metabolites and compounds in AcrAB
433 mutants could be toxic or at least disadvantageous at a given moment in *Photorhabdus* life cycle,

producing a negative feedback on the production of attributes directly or indirectly required to infect and colonize the host as also shown in *Salmonella* Typhimurium (Webber *et al.,* 2009; Heinrich *et al.,* 2017). In harmony with this, the slight virulence exaltation noted upon *acrAB* overexpression in mutant strains is suggestive of an enhanced production/export of yet unknown bacterial effectors/toxic compounds via the AcrAB pump, contributing to a better adaptation and survival to the complex stresses within the dying insect. Indeed, an *in vivo* metabolomic study of the Δ*acrAB* mutant would be interesting to argue this hypothesis.

In conclusion, we present compelling evidence in support of AcrAB as an essential efflux pump for intrinsic MDR of *P. laumondii* that also contributes to virulence in insects. It is likely that natural selection is aimed at maintaining AcrAB as the main polyselective RND efflux pump of *Photorhabdus* in order to improve bacterial resilience and versatility within its well-complicated life cycle. Further in-depth analyses of the AcrAB efflux pump in *P. laumondii* are ongoing so that the full characterization of its natural substrates could improve our knowledge about *Photorhabdus* dual interaction with its invertebrate hosts.

Experimental Procedures

Bacterial strains, plasmids and media

The bacterial strains and plasmids used in this study and their sources are listed in Table S2.

P. laumondii (Duchaud *et al.,* 2003) was routinely grown in LB broth (Difco) or on nutrient/LB agar (Difco) at 28˚C. *Escherichia coli* XLI-blue MRF' (Stratagene) and WM3064 (Paulick *et al.,* 2009) were routinely grown in LB broth or on LB agar at 37˚C. When required, the final concentrations of antibiotics used for the selection of *P. laumondii* mutants were: 8 or 15 µg.mL^{-1} for Chloramphenicol (Cm) and 10 µg.mL^{-1} for Kanamycin (Km). Similarly, Gentamicin (Gm) at 15 µg.mL^{-1} was added to cultures of strains harboring pJQ200SK and pBBR1-MCS5 derived

458 plasmids and Km at 20 µg.mL^{-1} was added when growing strains harboring pPROBE'-*gfp*[AAV]
459 and pPROBE-*gfp*[AAV] derived plasmids. Diaminopimelic acid (DAP) at 100 µg.mL^{-1} was added
460 to cultures of *E. coli* WM3064 strain auxotrophic for this amino acid. Other cultural characteristics
461 of *Photorhabdus* were revealed on nutrient bromothymol blue 2,3,5-triphenyltetrazolium chloride
462 agar (NBTA agar) as previously described (Akhurst, 1980).
463

464 **Molecular Genetic Techniques**
465 DNA manipulations were carried out as previously described (Abi Khattar *et al.,* 2019). Plasmids
466 were introduced into *E. coli* XLI blue MRF' or WM3064 by transformation and then transferred
467 to *P. laumondii* by conjugative mating (Mouammine *et al.,* 2017) using the donor *E. coli* WM3064
468 strain. All constructs were checked by sequencing at Eurofins Genomics (Germany). The primers
469 used in this study (IDT, Belgium) are described in Table S3.
470

471 **Sequence analysis of *acrR* from different *P. laumondii* strains newly isolated from nematodes**
472 Several *P. laumondii* strains were isolated from nematodes of our laboratory collection using Fast
473 Prep (MP Biomedical, LLC. Fast Prep -24™ 5G [V1.13]) as follows: a group of 20 nematodes
474 contained in 200 µL of LB broth were transferred to individual reaction tubes and grinded with
475 three glass beads at a homogenization speed of 4.5 ms^{-1} for two periods of 40 seconds. The mixture
476 was then centrifuged at 10,226 x *g* for 1 minute in order to pool all the contents to the bottom of
477 the reaction tube. 100 µL of this mixture were then plated onto nutrient agar and plates were
478 incubated at 28 °C for 48 hours. Screening for bioluminescent *Photorhabdus* colonies was
479 performed using LI-COR imaging system. The *acrR* gene was amplified by PCR from a total of 5
480 strains using iProof High-Fidelity PCR Kit (Biorad) and the L-*acrR*-seq and R-*acrR*-seq primers

(Table S3). These primers were designed in highly conserved regions after multiple nucleotide sequence alignment from different *Photorhabdus* strains. In order to detect possible mutation(s) in the *acrR* gene and/or its promoter region, the expected 791 bp PCR products were purified prior to direct sequencing and the obtained nucleotide sequences were analyzed by MultAlin software version 5.3.3.

Construction of the Δ*acrA*, Δ*mdtA*Δ*acrA* and Δ*acrA*-like *P. laumondii* mutants

Firstly, we constructed a pJQ-KmT1 plasmid using a 1080 bp PCR fragment containing a Km resistance gene from the pPROBE-AAV (using L-Km-SpeI and R-Km-PvuI primers) and a 924 bp PvuI-SalI fragment from the same pPROBE-AAV plasmid containing four *rrnB* T1 terminators cloned together in the SpeI and SalI sites of the pJQ200SK vector. The upstream and downstream regions of the *acrA* gene were then amplified by PCR with the appropriate primer pairs: J1-SacI / J2-SpeI (upstream) and J6-SalI / J7-ApaI (downstream) generating a 563 bp PCR1-*acrA* fragment and a 596 bp PCR2-*acrA* fragment, respectively (Table S3). Then, both fragments were cloned using the appropriate restriction sites: PCR2-*acrA* fragment was digested with SalI and ApaI and cloned in the same sites of the pJQ-KmT1 generating the pJQ-KmT1-PCR2 plasmid. The PCR1-*acrA* fragment was digested with SacI and SpeI and cloned in the same sites of pJQ-KmT1-PCR2 generating the pJQ-*acrA*-KmT1 plasmid. The final pJQ-*acrA*-KmT1 plasmid was introduced by mating into each of the *P. laumondii* TT01 WT and the corresponding Δ*mdtA* strains as previously described (Mouammine *et al.,* 2017). Allelic exchange experiments were carried out on the obtained exconjugants as previously described (Brillard *et al.,* 2002). Km^R and Sac^R exconjugants were selected on LB agar with 4% sucrose and kanamycin. The 658 bp *acrA* deletion and the KmT1 insertion were checked by PCR using the two primer pairs: L-verif-acrR / R-verif-acrB

amplifying 3.7 kb fragment, L-Km-SpeI / R-verif-acrB amplifying a 3 kb fragment (Table S3) and then confirmed by DNA sequencing (Eurofins Genomics). The resulting recombinant clones were named Δ*acrA* and Δ*mdtA*Δ*acrA*.

In the same way, the upstream and downstream regions of the *plu0759* gene were amplified by PCR with the appropriate primer pairs: BamHI-down-F-plu0759 / XbaI-down-R-plu0759 (upstream) and SacI-Up-F-plu0759 / BamHI-Up-R-plu0759 (downstream) generating a 719 bp PCR1-*acrA*-like fragment and a 625 bp PCR2-*acrA*-like fragment, respectively (Table S3). Then, the pJQ200SK suicide vector digested with SacI and XbaI, the PCR1-*acrA*-like digested with SacI and BamHI, the 3.726 kb-BamHI ΩCm fragment from pHP45-ΩCm, and the PCR2-*acrA*-like digested with BamHI and XbaI were ligated together generating the plasmid pJQ-*plu0759*-ΩCm. Allelic exchange experiments were then performed on the obtained exconjugants and the 524 bp *plu0759* deletion and ΩCm insertion were verified by PCR using the primers: L-verif-plu0758 / ΩCm-L2 / ΩCm-R2 yielding a 981 pb fragment (Table S3), and then confirmed by DNA sequencing (Eurofins Genomics). The resulting recombinant clone was named Δ*acrA*-like.

Vector constructions for complementation assays

The entire *acrAB* operon (*plu3851-plu3852*) of *P. laumondii* TT01 and *acrR* (*plu3850*) gene of all *P. laumondii* strains (https://www.mage.genoscope.cns.fr/agc/mage) used in this study were amplified by PCR from genomic DNA using iProof High-Fidelity PCR Kit (BioRad) and the respective primer pairs: PstI-acrA / SacI-acrB and KpnI-acrR-RBS-F harbouring the RBS of *phoP* gene from *P. laumondii* TT01 WT / BamHI-acrR-R. The resulting 4.6 kb *acrAB* and 642 bp *acrR* products were digested with PstI / SacI and KpnI / BamHI, respectively, and then cloned separately in the same restriction sites of the pBBR1-MCS5 vector. The pBBR1-*acrAB* plasmid was then

transferred into Δ*acrA* and Δ*mdtA*Δ*acrA* strains while the pBBR1-*acrR* plasmid was transferred into TT01 WT by mating (Mouammine *et al.,* 2017). Similarly, the empty vector pBBR1-MCS5 and pBBR1-*mdtABC* were transferred into the same strains as controls for complementation assays.

Construction and analysis of transcriptional fusions with the green fluorescent protein gene *gfp*[AAV]

The promoter regions of the *acrAB* (P_{acrA}) and *acrR* (P_{acrR}) genes were inserted upstream from a promoter-less *gfp*[AAV] gene located on the low-copy plasmids, pPROBE'-*gfp*[AAV] and pPROBE-*gfp*[AAV], respectively (Miller *et al.,* 2000), in order to generate the corresponding P_{acrA}-*gfp*'[AAV] and P_{acrR}-*gfp*[AAV] transcriptional fusions. Briefly, the 129 pb intergenic region located between the divergently transcribed *acrAB* and *acrR* genes and harboring their corresponding overlapped promoter sequences was PCR amplified from genomic DNA of *P. laumondii* with EcoRI-PacrA-L and BamHI-PacrA-R primers (Table S3). The PCR products were then digested with EcoRI and BamHI and cloned separately in the same restriction sites upstream from *gfp*[AAV] of each of the pPROBE'-*gfp*[AAV] and pPROBE-*gfp*[AAV] vectors generating respectively P_{acrR}-*gfp*[AAV] and P_{acrA}-*gfp*'[AAV]. These plasmids were introduced separately by mating into the *P. laumondii* TT01 WT as previously described (Mouammine *et al.,* 2017). The empty pPROBE-*gfp*[AAV] plasmid was also transferred into the same strain as negative controls while the TT01 strain carrying the P_{lac}–*gfp*[AAV] (Abi Khattar *et al.,* 2019) fusion was used as a positive control. Specific fluorescence kinetics in LB broth containing the appropriate kanamycin concentration were performed in black-sided clear bottomed 96-well plates (Greiner) after inoculating at 1/500 dilution of an overnight culture of one of the TT01 WT harboring pPROBE-

550 *gfp*[AAV], P_{acrA}-*gfp*'[AAV], P_{acrR}-*gfp*[AAV], or P_{lac}-*gfp*[AAV] plasmids. Plates were incubated
551 for 36 h at 28˚C, with orbital shaking, in an Infinite M200 microplate reader (Tecan). Absorbance
552 at 600 nm and GFP fluorescence intensity, with excitation at 485 ± 4.5 nm and emission at 520 ±
553 10 nm, were measured every 30 min. Specific fluorescence was obtained by dividing fluorescence
554 units by the absorbance value. Relative Fluorescence Units (RFUs) were determined by the ratio
555 of each P_{acrA}-*gfp*'[AAV], P_{acrR}-*gfp*[AAV], and the promoter less construct specific fluorescence
556 value to that of the constitutive P_{lac}-*gfp*[AAV] used as a control, in a given condition and at
557 maximum fluorescence intensity (Abi Khattar *et al.,* 2019).
558

559 **RNA preparation and quantitative RT-PCR analysis**

560 Total RNA was extracted from the different *P. laumondii* strains grown in LB broth until late
561 exponential phase (OD_{540} of 0.8-1) using the RNeasy miniprep kit (Qiagen) with a DNase I
562 treatment step. DNA contamination in RNA samples was assessed by carrying out a control PCR.
563 The quantity and quality of RNA were assessed using an Agilent 2100 Bioanalyzer with the RNA
564 6000 Nano LabChip kit. RT-qPCR were performed in two steps. cDNAs were synthesized as
565 previously described (Mouammine *et al.,* 2017) and qPCR was performed into the Light Cycler
566 480 system (Roche) in triplicate, with the SensiFAST SYBR® No-ROX kit (Bioline), with 1.25
567 µL of cDNA and 1.75 µL of a mixture containing 1 µM of specific gene primers for *acrA*, *acrB*,
568 *hha*, *acrR*, *gyrB* that was used as an internal control gene (Table S3). The amounts of PCR products
569 generated from standard curves were determined with serially diluted genomic DNA from WT *P.*
570 *laumondii* TT01. Gene expression data were analyzed as the relative quantification ratio of a target
571 gene versus the reference housekeeping gene *recA* between TT01/ pBBR1-MCS5 and TT01/

572 pBBR1-*acrR* or TT01 WT and *acrA* mutant strains using REST software 2009 as previously
573 described (Jubelin *et al.,* 2013).

574

575 **Determination of the minimum inhibitory concentrations (MICs) of toxic compounds**

576 Broth microdilution MIC testing was performed for the various bacterial strains according
577 to CLSI M100 (CLSI, 2017), using stock solutions of a wide range of antimicrobial compounds
578 including, antimicrobial peptides (AMPs): polymyxin B (50 $mg.mL^{-1}$, SIGMA), colistin (20
579 $mg.mL^{-1}$, SIGMA), cecropin A (500 $\mu g.mL^{-1}$, SIGMA), cecropin C of *Spodoptera frugiperda* (100
580 $\mu g.mL^{-1}$ (Duvic *et al*., 2012; Huot *et al*., 2019)); antibiotics: novobiocin (2 $mg.mL^{-1}$, SIGMA),
581 nalidixic acid (1.25 $mg.mL^{-1}$, SIGMA), erythromycin (20 $mg.mL^{-1}$, SIGMA), enrofloxacin (1.5
582 $mg.mL^{-1}$, SIGMA), cefuroxime (20 $mg.mL^{-1}$, SIGMA), norfloxacin (18 $mg.mL^{-1}$, SIGMA),
583 ciprofloxacin (1 $mg.mL^{-1}$, SIGMA), cefaclor (25 $mg.mL^{-1}$, SIGMA), ceftriaxone (5 $mg.mL^{-1}$,
584 SIGMA), aztreonam (25 $mg.mL^{-1}$, SIGMA); plant flavonoids: saponin (SAP) (200 $mg.mL^{-1}$,
585 SIGMA); detergents: sodium dodecyl sulfate (SDS) (100 $mg.mL^{-1}$, SIGMA); bile salts: sodium
586 deoxycholate (DOC) (125 $mg.mL^{-1}$, SIGMA); redox indicator: 2,3,5-triphenyltetrazolium chloride
587 (TTC) (10 $mg.mL^{-1}$, SIGMA); metals: zinc ($ZnSO_4$) (2 M, SIGMA), copper ($CuSO_4$) (2 M,
588 SIGMA), magnesium ($MgSO_4$) (2 M, SIGMA), ammonium ($(NH_4)_2SO_4$) (2 M, SIGMA); dyes:
589 bromothymol blue (BTB) (5 $mg.mL^{-1}$, SIGMA), ethidium bromide (EtBr) (10 $mg.mL^{-1}$, SIGMA)
590 and other compounds such as indole (100 $mg.mL^{-1}$, SIGMA) and uric acid (10 $mg.mL^{-1}$, SIGMA).
591 Briefly, antibiotics were added directly to 96-well microtiter plates by serial two-fold dilutions in
592 Mueller-Hinton broth (Biokar). We dispensed about 10^3 bacteria into each well. MICs were
593 determined visually after incubation at 28 °C for 48h.

594

595 ***In vivo* infection and pathology assays**

596 To evaluate virulence into insects, the late instar larvae of the noctuidae, *Spodoptera littoralis,*
597 were intra-haemocoelically injected with 10^3 bacteria of each TT01 WT, Δ*acrA,* Δ*mdtA*Δ*acrA*,
598 TT01/pBBR1-MCS5, Δ*acrA*/pBBR1-MCS5 and Δ*acrA*/pBBR1-*acrAB* as previously described
599 (Abi Khattar *et al.,* 2019). Statistical analyses were performed using the nonparametric Gehan's
600 generalized Wilcoxon test using SPSS version 18.0 (SPSS, Inc., Chicago, IL) for the comparison
601 of survival rates as previously described (Payelleville *et al.,* 2019). *In vivo* gene expression was
602 assessed after injecting between 10^4 and 5.10^4 bacteria harboring the corresponding *gfp*[AAV]
603 transcriptional fusions followed by haemolymph extraction and mid-gut connective tissue
604 dissection from scarified and dead insect larvae for examination, at regular intervals, under
605 fluorescence microscopy (Leica), as previously described (Abi Khattar *et al.,* 2019).
606

607 ## Acknowledgments

608 This work was funded by a research grant (2018-2020) from the Lebanese University. LH was
609 granted by a doctoral fellowship from the National Council for Scientific Research - Lebanon and
610 the University of Montpellier. We would like to thank Gaëtan Clabots, Raphaël Bousquet and
611 Clotilde Gibard for insect rearing and the quarantine insect platform (PIQ), member of the
612 Vectopole Sud network, for providing the infrastructure needed for pest insect experimentations,
613 Sylvie Pagès for SPSS statistical analyses of *in vivo* pathogenicity assays, and Jona Karam for the
614 construction of the pJQ-*acrA*-KmT1 plasmid. We also thank Philippe Clair from Montpellier
615 GenomiX facility for expert technical assistance with real-time PCR, and the Microbiology
616 laboratory of the LARI (Fanar Station) directed by Dr. Rima El Hage for their logistic support. All
617 authors have no conflict of interest to declare.

References

Abi Khattar, Z., Lanois, A., Hadchity, L., Gaudriault, S., and Givaudan, A. (2019) Spatiotemporal expression of the putative MdtABC efflux pump of *Phtotorhabdus luminescens* occurs in a protease-dependent manner during insect infection. *PLoS One* **14**: e0212077.

Adeolu, M., Alnajar, S., Naushad, S., and R, S.G. (2016) Genome-based phylogeny and taxonomy of the 'Enterobacteriales': proposal for Enterobacterales ord. nov. divided into the families *Enterobacteriaceae*, *Erwiniaceae* fam. nov., *Pectobacteriaceae* fam. nov., *Yersiniaceae* fam. nov., *Hafniaceae* fam. nov., *Morganellaceae* fam. nov., and *Budviciaceae* fam. nov. *Int J Syst Evol Microbiol* **66**: 5575-5599.

Akhurst, R.J. (1980) Morphological and Functional Dimorphism in *Xenorhabdus* spp., Bacteria Symbiotically Associated with the Insect Pathogenic Nematodes *Neoaplectana* and *Heterorhabditis*. *Journal of General Microbiology* **121**.

Alav, I., Sutton, J.M., and Rahman, K.M. (2018) Role of bacterial efflux pumps in biofilm formation. *J Antimicrob Chemother* **73**: 2003-2020.

Alcalde-Rico, M., Hernando-Amado, S., Blanco, P., and Martinez, J.L. (2016) Multidrug Efflux Pumps at the Crossroad between Antibiotic Resistance and Bacterial Virulence. *Front Microbiol* **7**: 1483.

Anes, J., McCusker, M.P., Fanning, S., and Martins, M. (2015) The ins and outs of RND efflux pumps in *Escherichia coli*. *Front Microbiol* **6**: 587.

Annunziato, G. (2019) Strategies to Overcome Antimicrobial Resistance (AMR) Making Use of Non-Essential Target Inhibitors: A Review *Int J Mol Sci* **20**.

Bailey, A.M., Ivens, A., Kingsley, R., Cottell, J.L., Wain, J., and Piddock, L.J. (2010) RamA, a member of the AraC/XylS family, influences both virulence and efflux in *Salmonella enterica* serovar Typhimurium. *J Bacteriol* **192**: 1607-1616.

Baucheron, S., Nishino, K., Monchaux, I., Canepa, S., Maurel, M.C., Coste, F. *et al*. (2014) Bile-mediated activation of the *acrAB* and *tolC* multidrug efflux genes occurs mainly through transcriptional derepression of *ramA* in *Salmonella enterica* serovar Typhimurium. *J Antimicrob Chemother* **69**: 2400-2406.

Bennett, H.P., and Clarke, D.J. (2005) The *pbgPE* operon in *Photorhabdus luminescens* is required for pathogenicity and symbiosis. *J Bacteriol* **187**: 77-84.

Bina, X.R., Provenzano, D., Nguyen, N., and Bina, J.E. (2008) *Vibrio cholerae* RND family efflux systems are required for antimicrobial resistance, optimal virulence factor production, and colonization of the infant mouse small intestine. *Infect Immun* **76**: 3595-3605.

Blair, J.M., Smith, H.E., Ricci, V., Lawler, A.J., Thompson, L.J., and Piddock, L.J. (2015) Expression of homologous RND efflux pump genes is dependent upon AcrB expression: implications for efflux and virulence inhibitor design. *J Antimicrob Chemother* **70**: 424-431.

Boemare, NE. (2002) Biology, Taxonomy and Systematics of *Photorhabdus* and *Xenorhabdus*. In *Entomopathogenic Nematology*. Gaugler, R. (ed). Wallingford, United Kingdom: CAB International pp. 35-56.

Brillard, J., Duchaud, E., Boemare, N., Kunst, F., and Givaudan, A. (2002) The PhlA hemolysin from the entomopathogenic bacterium *Photorhabdus luminescens* belongs to the two-partner secretion family of hemolysins. *J Bacteriol* **184**: 3871-3878.

Burse, A., Weingart, H., and Ullrich, M.S. (2004) The phytoalexin-inducible multidrug efflux pump AcrAB contributes to virulence in the fire blight pathogen, *Erwinia amylovora*. *Mol Plant Microbe Interact* **17**: 43-54.

663 Cauilan, A., Ramos, K., Harmon, D.E., and Ruiz, C. (2019) Global effect of the AcrAB-TolC
664 multidrug efflux pump of *Escherichia coli* in cell metabolism revealed by untargeted
665 metabolomics. *Int J Antimicrob Agents* **54**: 105-107.
666 Ciche, T.A., and Ensign, J.C. (2003) For the insect pathogen *Photorhabdus luminescens*, which
667 end of a nematode is out? *Appl Environ Microbiol* **69**: 1890-1897.
668 Clarke, D.J. (2020) *Photorhabdus*: a tale of contrasting interactions. *Microbiology*.
669 Clinical and Laboratory Standards Institute (CLSI). Performance Standards for Antimicrobial
670 Susceptibility Testing. CLSI Supplement M100 (27th ed.): CLSI, Wayne, PA (2017).
671 Colclough, A.L., Alav, I., Whittle, E.E., Pugh, H.L., Darby, E.M., Legood, S.W. *et al*. (2020) RND
672 efflux pumps in Gram-negative bacteria; regulation, structure and role in antibiotic resistance.
673 *Future Microbiol* **15**: 143-157.
674 Deng, W., Li, C., and Xie, J. (2013) The underling mechanism of bacterial TetR/AcrR family
675 transcriptional repressors. *Cell Signal* **25**: 1608-1613.
676 Derzelle, S., Turlin, E., Duchaud, E., Pages, S., Kunst, F., Givaudan, A., and Danchin, A. (2004)
677 The PhoP-PhoQ two-component regulatory system of *Photorhabdus luminescens* is essential
678 for virulence in insects. *J Bacteriol* **186**: 1270-1279.
679 Du, D., Wang-Kan, X., Neuberger, A., van Veen, H.W., Pos, K.M., Piddock, L.J.V., and Luisi,
680 B.F. (2018) Multidrug efflux pumps: structure, function and regulation. *Nat Rev Microbiol*
681 **16**: 523-539.
682 Duchaud, E., Rusniok, C., Frangeul, L., Buchrieser, C., Givaudan, A., Taourit, S. *et al*. (2003) The
683 genome sequence of the entomopathogenic bacterium *Photorhabdus luminescens*. *Nat*
684 *Biotechnol* **21**: 1307-1313.
685 Duval, V., and Lister, I.M. (2013) MarA, SoxS and Rob of *Escherichia coli* - Global regulators of
686 multidrug resistance, virulence and stress response. *Int J Biotechnol Wellness Ind* **2**: 101-124.
687 Duvic, B., Jouan, V., Essa, N., Girard, P.A., Pages, S., Abi Khattar, Z. *et al*. (2012) Cecropins as
688 a marker of *Spodoptera frugiperda* immunosuppression during entomopathogenic bacterial
689 challenge. *J Insect Physiol* **58**: 881-888.
690 Eleftherianos, I., ffrench-Constant, R.H., Clarke, D.J., Dowling, A.J., and Reynolds, S.E. (2010)
691 Dissecting the immune response to the entomopathogen *Photorhabdus*. *Trends Microbiol* **18**:
692 552-560.
693 European Committee on Antimicrobial Susceptibility Testing (EUCAST). Breakpoint tables for
694 interpretation of MICs and zone diameters. Version 11.0, 2021: http://www.eucast.org.
695 Heinrich, A.K., Hirschmann, M., Neubacher, N., and Bode, H.B. (2017) LuxS-dependent AI-2
696 production is not involved in global regulation of natural product biosynthesis in
697 *Photorhabdus* and *Xenorhabdus*. *PeerJ* **5**: e3471.
698 Horiyama, T., and Nishino, K. (2014) AcrB, AcrD, and MdtABC multidrug efflux systems are
699 involved in enterobactin export in *Escherichia coli*. *PLoS One* **9**: e108642.
700 Huot, L., George, S., Girard, P.A., Severac, D., Negre, N., and Duvic, B. (2019) *Spodoptera*
701 *frugiperda* transcriptional response to infestation by *Steinernema carpocapsae*. *Sci Rep* **9**:
702 12879.
703 Jaktaji, R.P., and Jazayeri, N. (2013) Expression of *acrA* and *acrB* Genes in *Esherichia coli*
704 Mutants with or without *marR* or *acrR* Mutations. *Iran J Basic Med Sci* **16**: 1254-1258.
705 Johnigk, S.A., and Hlers, R.U. (1999) Juvenile development and life cycle of *Heterorhabditis*
706 *bacteriophora* and *H. indica* (Nematoda:*Heterorhabditidae*) *Nematology* **1**: 251-260.
707 Joo, H.S., Fu, C.I., and Otto, M. (2016) Bacterial strategies of resistance to antimicrobial peptides.
708 *Philos Trans R Soc Lond B Biol Sci* **371**.

Jubelin, G., Lanois, A., Severac, D., Rialle, S., Longin, C., Gaudriault, S., and Givaudan, A. (2013) FliZ is a global regulatory protein affecting the expression of flagellar and virulence genes in individual *Xenorhabdus nematophila* bacterial cells. *PLoS Genet* **9**: e1003915.

Kang, H., and Gross, D.C. (2005) Characterization of a resistance-nodulation-cell division transporter system associated with the *syr-syp* genomic island of *Pseudomonas syringae* pv. *syringae*. *Appl Environ Microbiol* **71**: 5056-5065.

Kobayashi, A., Hirakawa, H., Hirata, T., Nishino, K., and Yamaguchi, A. (2006) Growth phase-dependent expression of drug exporters in *Escherichia coli* and its contribution to drug tolerance. *J Bacteriol* **188**: 5693-5703.

Kobylka, J., Kuth, M.S., Muller, R.T., Geertsma, E.R., and Pos, K.M. (2020) AcrB: a mean, keen, drug efflux machine. *Ann N Y Acad Sci* **1459**: 38-68.

Kunkle, D.E., Bina, X.R., and Bina, J.E. (2017) The *Vibrio cholerae* VexGH RND Efflux System Maintains Cellular Homeostasis by Effluxing Vibriobactin. *mBio* **8**.

Lee, J., and Zhang, L. (2015) The hierarchy quorum sensing network in *Pseudomonas aeruginosa*. *Protein Cell* **6**: 26-41.

Leus, I.V., Weeks, J.W., Bonifay, V., Smith, L., Richardson, S., and Zgurskaya, H.I. (2018) Substrate Specificities and Efflux Efficiencies of RND Efflux Pumps of *Acinetobacter baumannii*. *J Bacteriol* **200**.

Li, M., Gu, R., Su, C.C., Routh, M.D., Harris, K.C., Jewell, E.S. *et al*. (2007) Crystal structure of the transcriptional regulator AcrR from *Escherichia coli*. *J Mol Biol* **374**: 591-603.

Li, X.Z., and Nikaido, H. (2016) Antimicrobial Drug Efflux Pumps in *Escherichia coli*. In *Efflux-Mediated Antimicrobial Resistance in Bacteria*. Publishing, S.I. (ed). Switzerland Adis, Cham.

Machado, R.A.R., Wuthrich, D., Kuhnert, P., Arce, C.C.M., Thonen, L., Ruiz, C. *et al*. (2018) Whole-genome-based revisit of *Photorhabdus* phylogeny: proposal for the elevation of most *Photorhabdus* subspecies to the species level and description of one novel species *Photorhabdus bodei* sp. nov., and one novel subspecies *Photorhabdus laumondii* subsp. clarkei subsp. nov. *Int J Syst Evol Microbiol* **68**: 2664-2681.

Martinez, J.L., Sanchez, M.B., Martinez-Solano, L., Hernandez, A., Garmendia, L., Fajardo, A., and Alvarez-Ortega, C. (2009) Functional role of bacterial multidrug efflux pumps in microbial natural ecosystems. *FEMS Microbiol Rev* **33**: 430-449.

Miller, W.G., Leveau, J.H., and Lindow, S.E. (2000) Improved *gfp* and *inaZ* broad-host-range promoter-probe vectors. *Mol Plant Microbe Interact* **13**: 1243-1250.

Mira, A., Ochman, H., and Moran, N.A. (2001) Deletional bias and the evolution of bacterial genomes. *Trends Genet* **17**: 589-596.

Mouammine, A., Pages, S., Lanois, A., Gaudriault, S., Jubelin, G., Bonabaud, M. *et al*. (2017) An antimicrobial peptide-resistant minor subpopulation of *Photorhabdus luminescens* is responsible for virulence. *Sci Rep* **7**: 43670.

Nagakubo, S., Nishino, K., Hirata, T., and Yamaguchi, A. (2002) The putative response regulator BaeR stimulates multidrug resistance of *Escherichia coli* via a novel multidrug exporter system, MdtABC. *J Bacteriol* **184**: 4161-4167.

Nazarov, P.A., Sorochkina, A.I., and Karakozova, M.V. (2020) New Functional Criterion for Evaluation of Homologous MDR Pumps. *Front Microbiol* **11**: 592283.

Ni, R.T., Onishi, M., Mizusawa, M., Kitagawa, R., Kishino, T., Matsubara, F. *et al*. (2020) The role of RND-type efflux pumps in multidrug-resistant mutants of *Klebsiella pneumoniae*. *Sci Rep* **10**: 10876.

Nielsen-LeRoux, C., Gaudriault, S., Ramarao, N., Lereclus, D., and Givaudan, A. (2012) How the insect pathogen bacteria *Bacillus thuringiensis* and *Xenorhabdus*/*Photorhabdus* occupy their hosts. *Current Opinion in Microbiology* **15**: 220–231

Nishino, K. (2016) Antimicrobial Drug Efflux Pumps in *Salmonella*. In *Efflux-Mediated Antimicrobial Resistance in Bacteria*. Publishing, S.I. (ed). Switzerland: Adis, Cham.

Nishino, K., Latifi, T., and Groisman, E.A. (2006) Virulence and drug resistance roles of multidrug efflux systems of *Salmonella enterica* serovar Typhimurium. *Mol Microbiol* **59**: 126-141.

Olliver, A., Valle, M., Chaslus-Dancla, E., and Cloeckaert, A. (2004) Role of an *acrR* mutation in multidrug resistance of in vitro-selected fluoroquinolone-resistant mutants of *Salmonella enterica* serovar Typhimurium. *FEMS Microbiol Lett* **238**: 267-272.

Paulick, A., Koerdt, A., Lassak, J., Huntley, S., Wilms, I., Narberhaus, F., and Thormann, K.M. (2009) Two different stator systems drive a single polar flagellum in *Shewanella oneidensis* MR-1. *Mol Microbiol* **71**: 836-850.

Payelleville, A., Blackburn, D., Lanois, A., Pages, S., Cambon, M.C., Ginibre, N. *et al*. (2019) Role of the *Photorhabdus* Dam methyltransferase during interactions with its invertebrate hosts. *PLoS One* **14**: e0212655.

Pletzer, D., and Weingart, H. (2014) Characterization and regulation of the resistance-nodulation-cell division-type multidrug efflux pumps MdtABC and MdtUVW from the fire blight pathogen *Erwinia amylovora*. *BMC Microbiol* **14**: 185.

Rand, J.D., Danby, S.G., Greenway, D.L., and England, R.R. (2002) Increased expression of the multidrug efflux genes *acrAB* occurs during slow growth of *Escherichia coli*. *FEMS Microbiol Lett* **207**: 91-95.

Ren, Q., and Paulsen, I.T. (2005) Comparative analyses of fundamental differences in membrane transport capabilities in prokaryotes and eukaryotes. *PLoS Comput Biol* **1**: e27.

Ruiz, C., and Levy, S.B. (2014) Regulation of *acrAB* expression by cellular metabolites in *Escherichia coli*. *J Antimicrob Chemother* **69**: 390-399.

Stock, S.P., and Kaya, H.K. (1996) A multivariate analysis of morphometric characters of *Heterorhabditis* species (*Nemata*: *Heterorhabditidae*) and the role of morphometrics in the taxonomy of species of the genus. *J Parasitol* **82**: 806-813.

Strauch, O., and Ehlers, R.U. (1998) Food signal production of *Photorhabdus luminescens* inducing the recovery of entomopathogenic nematodes *Heterorhabditis* spp. in liquid culture. *Appl Microbiol Biotechnol* **50**: 369-374

Su, C.C., Rutherford, D.J., and Yu, E.W. (2007) Characterization of the multidrug efflux regulator AcrR from *Escherichia coli*. *Biochem Biophys Res Commun* **361**: 85-90.

Trimble, M.J., Mlynarcik, P., Kolar, M., and Hancock, R.E. (2016) Polymyxin: Alternative Mechanisms of Action and Resistance. *Cold Spring Harb Perspect Med* **6**.

Wang-Kan, X., Blair, J.M.A., Chirullo, B., Betts, J., La Ragione, R.M., Ivens, A. *et al*. (2017) Lack of AcrB Efflux Function Confers Loss of Virulence on *Salmonella enterica* Serovar Typhimurium. *mBio* **8**.

Webber, M.A., Talukder, A., and Piddock, L.J. (2005) Contribution of mutation at amino acid 45 of AcrR to *acrB* expression and ciprofloxacin resistance in clinical and veterinary *Escherichia coli* isolates. *Antimicrob Agents Chemother* **49**: 4390-4392.

Webber, M.A., Bailey, A.M., Blair, J.M., Morgan, E., Stevens, M.P., Hinton, J.C. *et al*. (2009) The global consequence of disruption of the AcrAB-TolC efflux pump in *Salmonella enterica* includes reduced expression of SPI-1 and other attributes required to infect the host. *J Bacteriol* **191**: 4276-4285.

801 Weston, N., Sharma, P., Ricci, V., and Piddock, L.J.V. (2018) Regulation of the AcrAB-TolC
802 efflux pump in *Enterobacteriaceae*. *Res Microbiol* **169**: 425-431.

803

804

805

806

Table 1. Growth patterns on modified NBTA media and minimum inhibitory concentrations (MICs) of BTB and TTC for the *P. laumondii* TT01 WT and its derivative strains.

Strains	Growth pattern			MICs [a] (µg.mL^{-1})	
	NA+BTB+TTC	NA+ BTB	NA+TTC	BTB	TTC
TT01 WT	+	+	+	>1250	1250
Δ*acrA*-like	+	+	+	>1250	1250
TT01/pBBR1-MCS5	+	+	+	625	1250
Δ*acrA*/pBBR1-MCS5	-	w	w	78	156
Δ*acrA*/pBBR1-*acrAB*	+	+	+	625	1250
Δ*acrA*/pBBR1-*mdtABC*	w	+	w	625	156
Δ*mdtA*Δ*acrA*/pBBR1-MCS5	-	-	w	20	156
Δ*mdtA*Δ*acrA*/pBBR1-*acrAB*	+	+	+	625	1250
Δ*mdtA*Δ*acrA*/pBBR1-*mdtABC*	w	+	w	625	156

NA: Nutrient agar; BTB: bromothymol blue; TTC: triphenyltetrazolium chloride; +: growth; -: no growth; w: weak.

[a] As determined by the broth dilution method (at least three replicates). MICs were scored after 48 hours of incubation at 28˚C. Standard deviations were equal to 0.

Table 2. Minimum inhibitory concentrations (MICs) of various antimicrobial compounds for different strains of *P. laumondii* TT01.

Antimicrobial compounds		MICs [a] (µg.mL^{-1}) of *P. laumondii* strains						
		TT01 WT	Δ*acrA*-like	TT01/ pBBR1-MCS5	Δ*acrA*/ pBBR1-MCS5	Δ*acrA*/ pBBR1-*acrAB*	Δ*mdtA*Δ*acrA*/ pBBR1-MCS5	Δ*mdtA*Δ*acrA*/ pBBR1-*acrAB*
Lipophilic drugs/Antibiotics	**Novo**	8	8	2	0.1	2	0.01	2
	Ery	78	78	63	2	63	1	63
AMPs	**Poly B**	6250	6250	6250	781	3125	391	3125
	Colistin	>5000	5000	>5000	625	2500	625	>5000
	Cec A	>125	ND	>125	>125	>125	>125	>125
	Cec C	>25	ND	>25	>25	>25	>25	>25
Bile salts	**DOC**	>31250	>31250	>31250	122	>31250	15	>31250
Detergents	**SDS**	313	313	313	10	313	10	313
Dyes	**EtBr**	63	63	31	0.5	31	0.5	31

Novo: novobiocin, Ery: erythromycin; Poly B: polymyxin B; Cec A: cecropin A; Cec C: cecropin C; DOC: deoxycholate; SDS: sodium dodecyl sulfate; EtBr: ethidium bromide; ND: not determined.

[a] As determined by the broth dilution method (at least three replicates). MICs were scored after 48 hours of incubation at 28˚C. Standard deviations were equal to 0.

Table 3. Minimum inhibitory concentrations (MICs) of various compounds for *P. laumondii* TT01 harbouring pBBR1-MCS5 or pBBR1-*acrR* plasmids.

Antimicrobial compounds		MICs [a] (µg.mL^{-1}) for *P. laumondii* strains	
		TT01/ pBBR1-MCS5	TT01/ pBBR1-*acrR*
Lipophilic drugs/Antibiotics	Novo	2	1
	Ery	63	63
Bile-salts	DOC	>31250	>31250
Detergents	SDS	313	313
Dyes	BTB	625	625
	TTC	1250	625

Novo: novobiocin;, Ery: erythromycin; Poly B: polymyxin B; DOC: deoxycholate; SDS: sodium dodecyl sulfate; BTB: bromothymol blue and TTC: triphenyl tetrazolium chloride.

[a] As determined by the broth dilution method (at least three replicates). MICs were scored after 48 hours of incubation at 28˚C. Standard deviations were equal to 0.

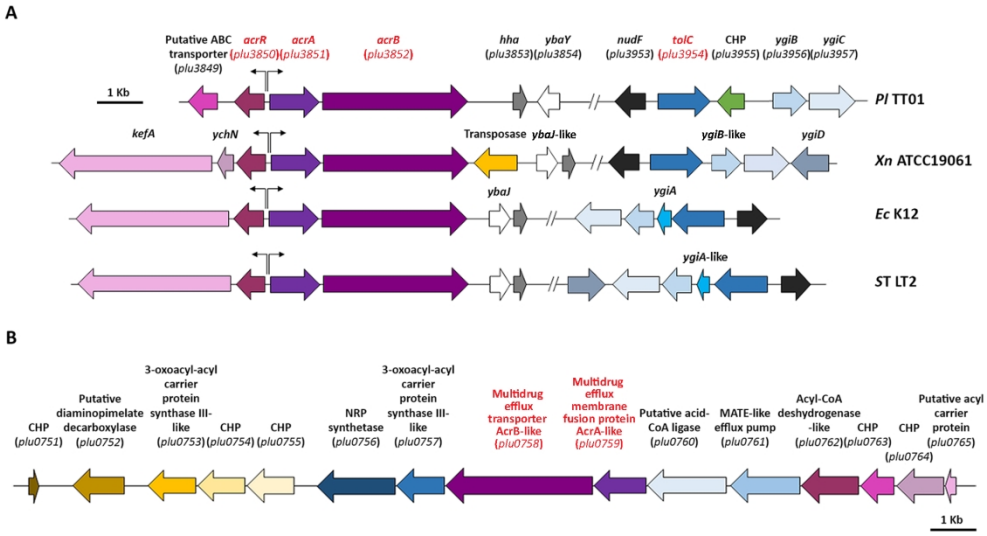

Fig. 1. Genomic environment of the acrRAB-tolC and *acrAB*-like loci in *P. laumondii* and other phylogenetically related bacteria. (A) Genomic organization of *acrRAB* and *tolC* loci in *P. laumondii* TT01, *X. nematophila* ATCC19061, *E. coli* K12 and *S. Typhimurium* LT2. (B) The *plu0751-plu0765* gene cluster in *P. laumondii* TT01. Genomic sequences and gene mapping in all strains shown were obtained from MaGe genoscope (https://www.mage.genoscope.cns.fr/agc/mage). *Pl: P. laumondii, Xn: X. nematophila, Ec: E. coli*, *S*T: *S.* Typhimurium and CHP: conserved hypothetical protein.

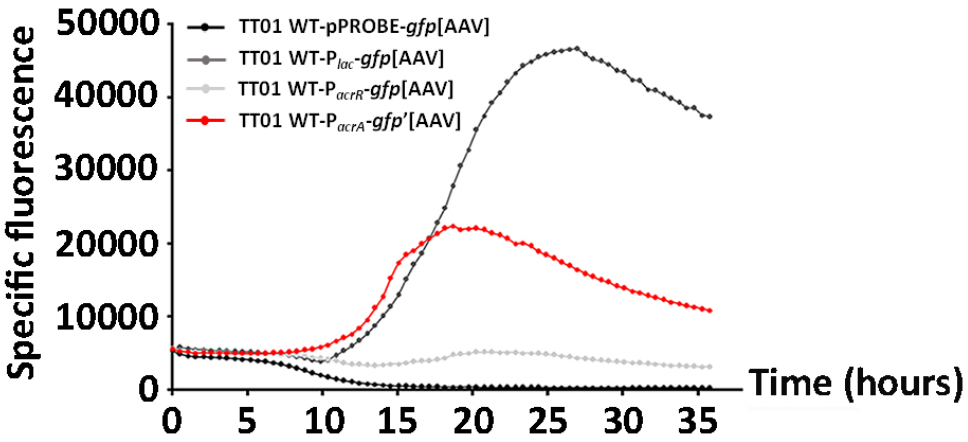

Fig. 2. Comparative expression levels of P_{acrA}-*gfp'*[AAV] and P_{acrR}-*gfp*[AAV] transcriptional fusions under regular laboratory growth conditions. TT01 WT strain carrying the P_{acrA}-*gfp'*[AAV] (red line), P_{acrR}-*gfp*[AAV] (light grey line), pPROBE-*gfp*[AAV] (black line) or P_{lac}-*gfp*[AAV] (dark grey line) transcriptional fusions were grown in LB medium and incubated for 36 hours at 28°C, with orbital shaking, in an Infinite M200 microplate reader (Tecan). Specific fluorescence values for each strain are expressed as the ratio of GFP fluorescence unit (FU) to A600nm value at a given time point.

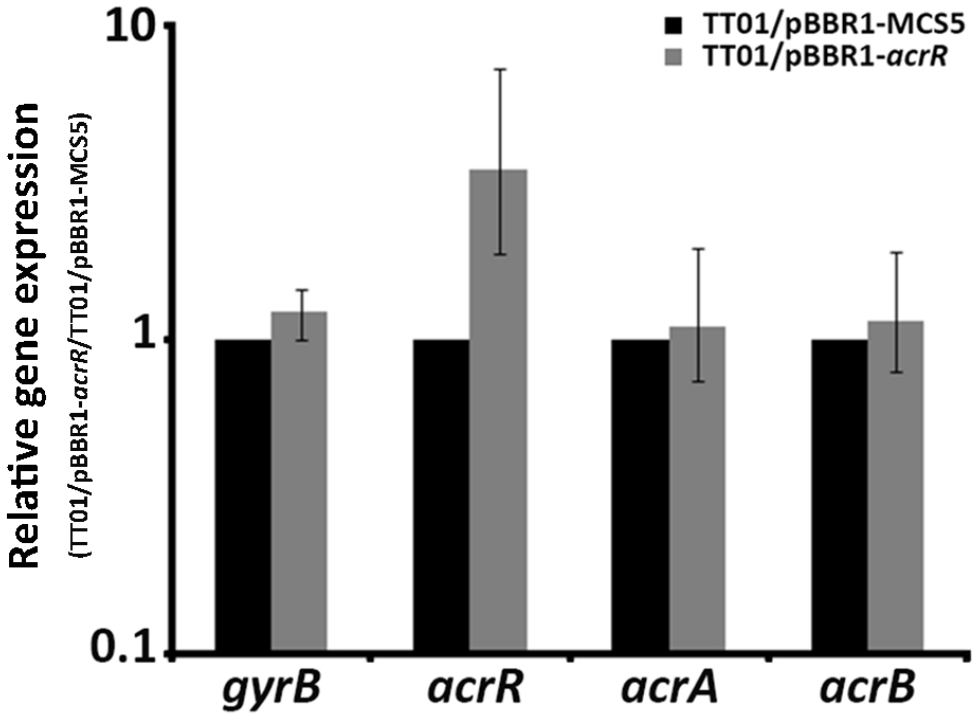

Fig. 3. AcrR-independent *acrAB* expression during the late exponential phase of growth under routine growth conditions. Total RNA was extracted from *P. laumondii* TT01 strains harboring pBBR1-MCS5 or pBBR1-*acrR* grown to late exponential phase in LB broth (OD_{540} of 0.8-1). Histograms represent the relative quantification ratio of a target gene (*gyrB* [internal control gene], *acrR, acrA* or *acrB*) versus the reference housekeeping gene *recA* between TT01/pBBR1-MCS5 and TT01/pBBR1-*acrR*. Data shown are the medians of three independent experiments and indicate statistically significant differences ($P < 0.05$) (REST software 2009).

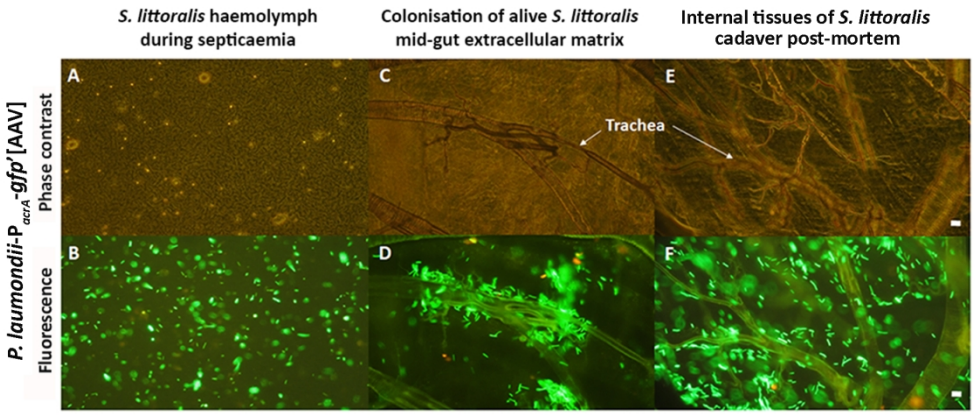

Fig. 4. *In vivo* expression of *P. laumondii acrAB* operon. Fluorescence monitoring of the *acrA* promoter activity was carried out in haemolymph during septicaemia (A and B), midgut connective tissue colonization (C and D) and within the cadaver of *Spodoptera littoralis* during the early post-mortem period (E and F). Insects were injected with recombinant *P. laumondii*-P$_{acrA}$-*gfp'*[AAV], then haemolymph and mid-gut connective tissues were regularly extracted upon septicaemia establishment, observed using phase contrast (A, C and E) and fluorescence (B, D and F) microscopy. Observations shown were made at 20 to 24 hours post-injection (for haemolymph and early septicaemia) and up to 28 hours post-injection for connective tissues, and correspond to the results of at least three independent experiments. Scale bar represents 10 µm.

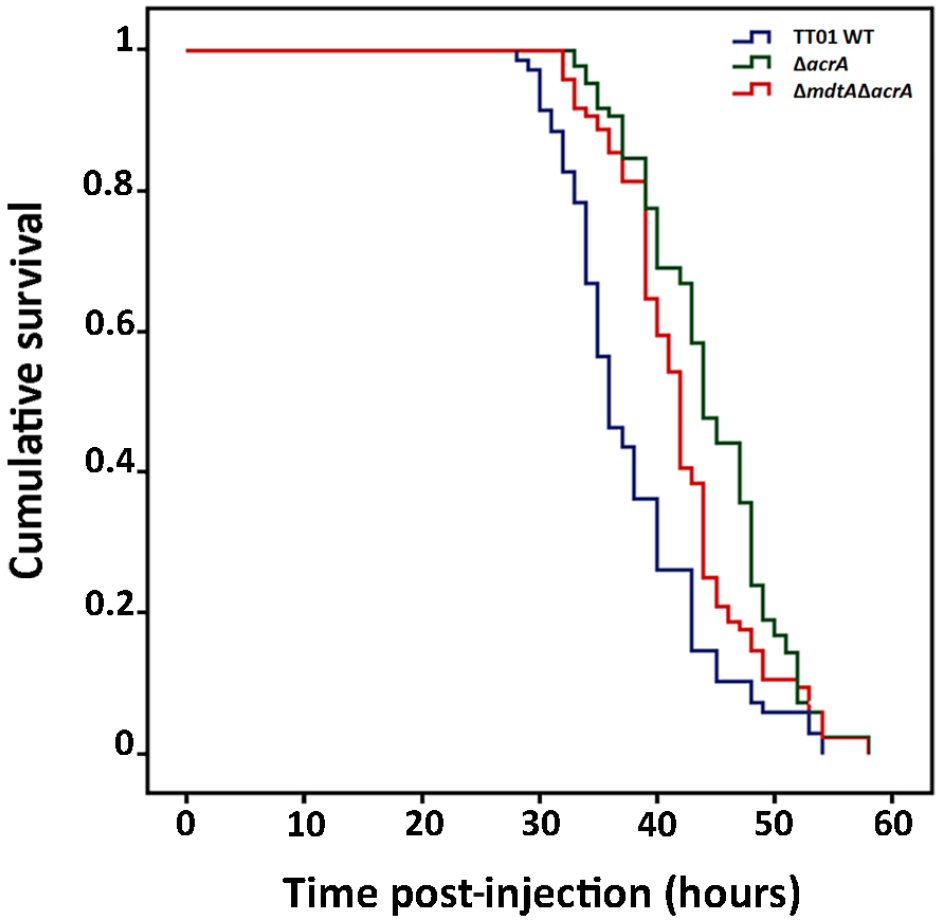

Fig. 5. Mortality rate of *Spodoptera littoralis* insect larvae after injection of the *P. laumondii* TT01 WT and its derivative mutant strains. Data shown are the means of three independent experiments as analyzed by Gehan's generalized Wilcoxon test using SPSS version 18.0 (SPSS, Inc., Chicago, IL) statistical analyses.